Cerebral Blood Flow Velocity and Periventricular White Matter Hyperintensities in Type 2 Diabetes

Published in final edited form as:
Diabetes Care. 2006 July ; 29(7): 1529–1534.

Cerebral Blood Flow Velocity and Periventricular White Matter Hyperintensities in Type 2 Diabetes

Vera Novak, MD, PHD[1], **David Last, PHD**[1], **David C. Alsop, PHD**[2], **Amir M. Abduljalil, PHD**[3], **Kun Hu, PHD**[1], **Lukas Lepicovsky**[1], **Jerry Cavallerano, OD, PHD**[4], and **Lewis A. Lipsitz, MD**[1,5]

1*From the Division of Gerontology, Beth Israel Deaconess Medical Center, Harvard Medical School, Boston, Massachusetts*

2*From the Department of Radiology, Beth Israel Deaconess Medical Center, Harvard Medical School, Boston, Massachusetts*

3*From the Department of Radiology, The Ohio State University, Columbus, Ohio*

4*From the Beetham Eye Institute, Joslin Diabetes Center, Boston, Massachusetts*

5*From the Hebrew SeniorLife, Boston, Massachusetts.*

Abstract

OBJECTIVE—Diabetes increases the risk for cerebromicrovascular disease, possibly through its effects on blood flow regulation. The aim of this study was to assess the effects of type 2 diabetes on blood flow velocities (BFVs) in the middle cerebral arteries and to determine the relationship between white matter hyperintensities (WMHs) on magnetic resonance imaging (MRI) and BFVs.

RESEARCH DESIGN AND METHODS—We measured BFVs in 28 type 2 diabetic and 22 control subjects (aged 62.3 ± 7.2 years) using transcranial Doppler ultrasound during baseline, hyperventilation, and CO_2 rebreathing. WMHs were graded, and their volume was quantified from fluid-attenuated inversion recovery images on a 3.0 Tesla MRI.

RESULTS—The diabetic group demonstrated decreased mean BFVs and increased cerebrovascular resistance during baseline, hypo- and hypercapnia ($P < 0.0001$), and impaired CO_2 reactivity ($P = 0.05$). WMH volume was negatively correlated with baseline BFV ($P < 0.0001$). A regression model revealed that baseline BFVs were negatively associated with periventricular WMHs, HbA_{1c} (A1C), and inflammatory markers and positively associated with systolic blood pressure ($R^2 = 0.86$, $P < 0.0001$).

CONCLUSIONS—Microvascular disease in type 2 diabetes, which manifests as white matter abnormalities on MRI, is associated with reduced cerebral BFVs, increased resistance in middle cerebral arteries, and inflammation. These findings are clinically relevant as a potential mechanism for cerebrovascular disease in elderly with type 2 diabetes.

Diabetes is a complex metabolic syndrome that increases the risk for vascular dementia (1) and stroke. Cerebral microvascular disease in diabetes has been attributed to the effects of chronic hyperglycemia on capillary structure (2), endothelial reactivity (3), and blood-brain

Address correspondence and reprint requests to Vera Novak, Division of Gerontology, Beth Israel Deaconess Medical Center, 110 Francis St., Boston, MA 02215. E-mail: vnovak@bidmc.harvard.edu.

D.C.A. has received research grant support from General Electric Healthcare Technologies.

A table elsewhere in this issue shows conventional and Système International (SI) units and conversion factors for many substances.

The costs of publication of this article were defrayed in part by the payment of page charges. This article must therefore be hereby marked "advertisement" in accordance with 18 U.S.C. Section 1734 solely to indicate this fact.

barrier permeability, thus affecting regional metabolism and blood flow regulation (4). Xenon blood flow (5) and transcranial Doppler ultrasound (TCD) studies indicate that patients with type 2 diabetes have impaired cerebrovascular reactivity to hypercapnia (6,7). Sub-cortical white matter hyperintensities (WMHs), which are seen as multifocal and diffuse areas of hyperintensity on T2-weighted magnetic resonance imaging (MRI) (8), are strongly associated with diabetes, hypertension, and other cardiovascular risk factors (9,10). WMHs have been prospectively linked to dementia, functional decline, and silent infarcts (9,11); therefore, WMHs may be manifestations of clinically significant cerebral microvascular disease.

We aimed to determine whether there is an independent relationship between white matter abnormalities on MRI and cerebral blood flow velocities (BFVs) in older adults with type 2 diabetes.

RESEARCH DESIGN AND METHODS

TCD and MRI studies were conducted in the SAFE (Syncope and Falls in the Elderly) Laboratory and at the Magnetic Resonance Imaging Center at the Beth Israel Deaconess Medical Center using a General Electric 3.0 Tesla VHI scanner. All subjects were recruited consecutively and provided informed consent approved by the institutional review boards at the Beth Israel Deaconess Medical Center and the Joslin Diabetes Center. Demographic and clinical characteristics are summarized in Table 1. The diabetic group consisted of 28 patients (16 men and 12 women) with type 2 diabetes (duration 2.8 ± 11.5 years; means ± SD). The control group consisted of 22 healthy subjects (12 men and 10 women) who were normotensive, had normal HbA_{1c} (A1C) levels, and were not treated for any systemic disease. All subjects were screened with a medical history, physical examination, and standard battery of autonomic tests (12). Laboratory chemistries included routine glucose, A1C, lipid and renal panels, differential white blood cell count (WBC), and urine chemistry panel. Soluble intracellular adhesion molecule-1 (sICAM-1), soluble vascular adhesion molecule, endothelin-1, and human interleukin-6 were measured from venous blood samples using the quantitative sandwich enzyme immunoassay technique (R & D Systems, Minneapolis, MN). C-reactive protein (CRP) was measured using high-sensitivity CRP assay Immulite-1000 (Diagnostic Product, Los Angeles, CA). Diabetic retinopathy was diagnosed in 10 diabetic patients with the Joslin Vision Network video-digital retinal imaging system, which uses a nonmydriatic retinal fundus camera that has been optimized for low–light level imaging without pupil dilatation (13) and has been validated against clinical examination and standard retinal imaging (14).

Subjects with a history of stroke, clinically important cardiac disease, arrhythmia, significant nephropathy, kidney or liver transplant, renal or congestive heart failure, uncontrolled hypertension, carotid artery stenosis >50% by medical history and magnetic resonance angiography, and neurological or other systemic disorders were excluded. Diabetic subjects were treated with insulin (9), oral glucose-control agents (12), or diet (7). In 10 hypertensive diabetic subjects (10), antihypertensive medications were discontinued for 3 days before the study. Medications affecting autonomic function and stimulants were not allowed before the study, but hypoglycemic agents and anticoagulants were allowed. Studies using the 3.0 Tesla MRI were completed in 17 control and 24 diabetic subjects. Subjects with metal implants, pacemakers, arterial stents, and claustrophobia were excluded.

Transcranial Doppler ultrasonography

TCD studies were conducted at least 2 h after the last meal according to the following protocol. The subjects rested supine for 10 min with continuous monitoring of cardiovascular, cerebrovascular, and respiratory signals in order to establish a baseline. The subjects hyperventilated to reduce CO_2 to 25 mmHg for 3 min. Then the subjects breathed a mixture

of 5% CO_2 and 95% air from a rebreathing bag to increase CO_2 up to 45 mmHg for 3 min, followed by a 5-min rest.

The middle cerebral arteries (MCAs), right (MCAr) and left (MCAl), were insonated from the temporal windows with 2-MHz probes using a TCD system (MultiDop X4; Neuroscan, Sterling, VA). Each probe was positioned to record the maximal BFVs and stabilized using a 3-D positioning system. Assumptions that MCA diameter (15) does not change must be made in order to relate BFV to blood flow. The electrocardiogram was measured from a modified lead II or III using a Spacelab monitor (SpaceLab Medical, Issaquah, WA). Beat-to-beat blood pressure was recorded from a finger with a Finapres device (Ohmeda Monitoring Systems, Englewood, CO) that reliably tracks intraarterial blood pressure when controlled for finger position and temperature (16) and was verified by arterial tonometry. Respiration and end-tidal CO_2 were measured from a mask using an infrared end-tidal volume monitor (Datex Ohmeda, Madison, WI).

Data acquisition and analysis

Electrocardiogram, blood pressure, BFV, respiration, and CO_2 analog signals were continuously acquired at 500 Hz using Labview 6.0 NIDAQ (National Instruments, Austin, TX). Heartbeat intervals were extracted using a peak detection algorithm, and occasional extrasystoles were removed using linear interpolation. Systolic, diastolic, and mean BFVs were detected from the envelope of the arterial flow waveforms for each heartbeat interval. Beat-to-beat values were averaged over baseline, hyperventilation, and CO_2 rebreathing. A 30-s average was also calculated for the BFV minimum during hyperventilation and maximum during CO_2 rebreathing. CO_2 reactivity was calculated as a slope of the linear regression of mean BFV and CO_2 between hyperventilation and CO_2 rebreathing. Vasodilatation and vasoconstriction reserves were calculated as the percent increment of mean BFV from baseline to the CO_2 rebreathing maximum and to the hyperventilation minimum. Cerebrovascular resistance (CVR) was calculated as the mean blood pressure divided by the mean BFV.

MRI sequences

Anatomical images (T1-weighted inversion recovery fast gradient-recalled echo [IR-FGR], fluid-attenuation inversion recovery [FLAIR], and dual T2-weighted fast spin echo) and 3-D magnetic resonance time-of-flight angiography were acquired using a General Electric 3.0 Tesla VHI scanner with quadrature head coil.

Image analysis

Periventricular WMHs present as hyperintense areas with >30% increase in signal intensity on T2-weighted images compared with adjacent white matter. Punctuate lesions are well-defined areas of >2 mm with high signal characteristics (10). FLAIR images were scored using a scale of 0–3 (0, no lesions; 1, focal; 2, beginning confluence; and 3, diffuse involvement of the entire region). Periventricular WMHs and punctuate lesions were graded on all slices in the anterior, middle, and posterior cerebral artery distributions and quantified as a sum, mean, and maximum grade. High-resolution T2-weighted FLAIR images were segmented using the thresholding of hyperintense pixels and a region growing method that allowed an accurate WMH detection without expertise. The brain tissue volumes were computed from the IR-FGR image using the Brain Extraction Tools algorithm (17) based on the expectation-maximization segmentation method (18,19) and was validated using a phantom model (20). The IR-FGR segmented image was registered on the FLAIR image (21) to compute the whole brain and gray and white matter volumes with the same resolution as WMHs and to normalize WMHs for the total brain volume. The graders who processed and scored images were masked to the subject and group assignments.

Statistical analysis

Descriptive statistics were used to summarize all variables. Physiological measurements were compared between the control and diabetic groups and among conditions (baseline, hyperventilation, and CO_2 rebreathing) using multivariate ANOVA with multiple measure adjustments and Wilk's λ post hoc tests. Oneway ANOVA and Fisher's exact test were used for nonrepeated variables. The χ^2 test was used to compare WMH distribution. Stepwise linear and logistic regression models were used to determine the relationships between WMHs and the average resting mean BFVs in both MCAs. The effects of group (control vs. diabetic), BMI, baseline systolic blood pressure, A1C, lipids, inflammation markers, and age and their interactions with other variables were also investigated. The effects of WMHs on CVR and CO_2 reactivity were evaluated using the same approach.

RESULTS

Demographic and laboratory measures

Table 1 compares the demographic, clinical, and biochemical characteristics between the control and diabetic groups. The diabetic group had significantly higher BMI, glucose, A1C, and triglycerides but had lower total, LDL, and HDL cholesterol. Diabetes was not controlled in 18 subjects (A1C 8.1 ± 1.2%). Inflammatory markers such as sICAM-1 ($P < 0.05$) and WBC ($P < 0.003$) were elevated in the diabetic group, but soluble vascular adhesion molecule-1, endothelin-1, CRP, and interleukin-6 levels were not different.

Transcranial Doppler study

As shown in Fig. 1, diabetes had significant effects on mean BFV and CVR in MCAr and MCAl during supine baseline, hyperventilation, and CO_2 rebreathing. Across all conditions, mean BFVs in both MCAs were lower in the diabetic compared with the control group ($P < 0.0001$; Fig. 1A and B). For each condition, BFVs were lower in the diabetic group during baseline (MCAr and MCAl, respectively: systolic BFV $P = 0.006$ and 0.05, diastolic BFV $P = 0.04$ and 0.005, and mean BFV $P = 0.005$ and 0.01), hyperventilation minimum (MCAr systolic $P = 0.02$, MCAl diastolic $P = 0.02$, and mean $P = 0.04$), and CO_2 rebreathing maximum (MCAr and MCAl, respectively: systolic $P = 0.003$ and 0.007, diastolic $P = 0.01$ and 0.002, and mean $P = 0.004$ and 0.006) (Fig. 1A and B). CVR was significantly higher in the diabetic group in all conditions in both MCAs (Fig. 1C and D). Heart rate ($P = 0.03$) and systolic blood pressure ($P = 0.03$) were higher in the diabetic group during baseline. CVR was positively associated with WMHs normalized for brain volume ($P < 0.0001$) and with A1C and BMI ($P < 0.0004$) ($R^2 = 0.83$, $P < 0.0001$). Mean BFVs in both MCAs, blood pressure, and CVR were not different between hypertensive and normotensive diabetic subjects in all conditions. There was a trend suggesting that autonomic neuropathy may affect mean BFV values ($P = 0.052$).

CO_2 reactivity was reduced in the diabetic group ($P = 0.05$) (Table 1) and was negatively associated with glucose ($P = 0.01$), diabetic retinopathy ($P = 0.02$), and normalized WMH volume ($R^2 = 0.54$, $P = 0.03$).

WMHs on MRI

Figure 2 is an example of WMH segmentation on axial FLAIR slices at the level of the ventricles for a control (Fig. 2A-C) and a diabetic (Fig. 2C-E) subject. The distribution of periventricular WMHs differed between the diabetic and control groups ($P < 0.0001$) and among the frontal, temporal, and parieto-occipital regions ($P < 0.0001$). Mean WMH grade in the frontal area was greater in the diabetic than in the control group (mean 0.09 ± 0.3 vs. 1.8 ± 0.4, $P = 0.01$) and was borderline in the parieto-occipital area in the diabetic group ($P < 0.07$).

Periventricular and punctuate WMH volume (5.9 ± 5.5 vs. 6.7 ± 5.4 cm^3) and WMH volume normalized for brain volume (0.7 ± 0.7 vs. 0.9 ± 0.7%) and for white matter volume (2.1 ± 1.9 vs. 2.5 ± 2.0%) were not different between the diabetic versus control group, respectively. Hypertensive diabetic subjects had a greater periventricular WMH grade ($P = 0.02$) and a greater number of subcortical punctuate WMHs (left temporal $P = 0.01$, basal ganglia $P = 0.02$) than normotensive diabetic subjects, but WMH volume was not different. Magnetic resonance angiography was normal. Brain volumes and diameters of MCAs and internal carotid artery diameters were comparable.

Multiple regression analysis

The total periventricular WMH grade was associated with reduced mean BFV in both groups ($P = 0.0002$; Fig. 3A). The total WMH volume ($P = 0.001$; Fig. 3B) and percentage of WMH volume normalized for brain volume ($P = 0.0006$) were negatively associated with mean BFV. We found excellent correlations between the total WMH grade (sum of all continuous and punctuate WMHs on the visual rating scale) and the WMH volume measured on FLAIR images ($P < 0.0001$; Fig. 3C), thus validating visual WMH rating using the quantitative volumetric WMH measures.

We assessed an independent relationship between WMH and mean BFV during baseline and determined contributions of type 2 diabetes and other risk factors. Mean baseline BFV was negatively associated with periventricular WMH ($P < 0.0001$) or normalized WMH volume ($P < 0.0001$) and uncontrolled diabetes, as indicated by A1C ($P = 0.01$), WBC ($P = 0.05$), and sICAM-1 ($P = 0.03$), and was positively associated with baseline systolic blood pressure ($P = 0.004$) (whole model $R^2 = 0.86$, $P < 0.0001$). This model was controlled for the effects of age and BMI. CRP was negatively correlated with mean BFV ($P = 0.008$) but positively associated with age ($P = 0.01$), BMI ($P = 0.003$), and WBC ($P = 0.01$).

CONCLUSIONS

Type 2 diabetes exerts complex effects on cerebral microvasculature that may alter cerebral blood flow regulation. We found a decrease of mean BFV and an increase of CVR in type 2 diabetic patients during baseline, hypocapnia, and hypercapnia. Baseline mean BFV was negatively associated with periventricular WMH grade and volume on T2-weighted images and with A1C and inflammation markers. WMHs were also linked with uncontrolled diabetes, elevated CVR, and impaired CO_2 reactivity. The relationship between WMH, uncontrolled diabetes and reduced BFV is of clinical relevance as a potential mechanism for cerebrovascular disease in elderly with type 2 diabetes.

Aging is associated with brain atrophy, changes in frontal subcortical white matter, and executive cognitive dysfunction (9). The CO_2 reactivity diminishes with age, uncontrolled diabetes, and risk factors for atherosclerosis (22). In community-living elderly people, blood flow in the WMHs was lower compared with normal-appearing white matter but flow augmentation to acetazolomide was preserved (23). Correlations among periventricular hyperintensities, demyelination, astrocytic gliosis, and dilatation of perivascular spaces support the theory of arteriosclerosis (8). Diabetic angiopathy is characterized by the vessel wall remodeling, media hypertrophy and increased stiffness (24) that may be enhanced by circulating vasoconstrictors and vascular inflammation. Diabetic subjects had impaired vasodilatation to hypercapnia, but vasoconstriction to hypocapnia was preserved. The MCA diameter was comparable between the groups, similarly to other human (25) and animal (24) studies.

Diabetes alters the glucose and insulin transfer across the blood-brain barrier (26,27), thus affecting regional metabolism and microcirculation (4). Chronic hyperglycemia, which further

alters membrane permeability (26,27) and decreases regional blood flow, may lead to permanent cell damage (25). Therefore, diabetes seems to be associated with progressive metabolic disturbance in the cerebrovascular bed that may affect blood flow and accelerate the white matter degeneration. Elevated sICAM-1 and WBC levels in the diabetic group, as well as a negative correlation between BFV with CRP and inflammation markers, support the notion of an active arteriosclerotic process affecting the cerebrovascular bed. An elevation of tumor necrosis factor-α and sICAM-1 accompanied retinal neuronal cell death and blood-brain barrier breakdown induced by oxidative stress in experimental diabetes (28). Tumor necrosis factor-α, which depresses endothelium-dependent vasorelaxation, was increased in diabetic patients with microangiopathy, indicating a relationship between endothelium dysfunction and suppressed production of endothelium-derived nitric oxide (29,30). Furthermore, elevated plasma hemostatic and inflammation markers may reflect insulin resistance and endothelial dysfunction antecedent to diabetes (31,32).

This study addressed an important question about the relationship between WMHs on MRI and BFVs in older adults with type 2 diabetes. It provided further evidence that type 2 diabetes is associated with microvascular disease that may reduce cerebral blood flow in elderly people. Interventions to treat microvascular disease and to enhance cerebral blood flow may play an important role in preventing cerebrovascular complications of diabetes. Future prospective studies are needed to determine whether low cerebral blood flow is a cause or effect of white matter disease.

Acknowledgments

This study was supported by American Diabetes Association Grant 1-03-CR-23 to V. N., National Institutes of Health (NIH) Older American Independence Center Grant 2P60 AG08812, NIH Program project AG004390, and General Clinical Research Center (GCRC) Grant MO1-RR01032.

We acknowledge the contributions of C. Kantor, BA; R.P. Marquis, BS; A. Tolson, BA; H.-C. Li, PhD; M. Munshi, MD; and the GCRC staff.

Abbreviations

BFV, blood flow velocity; CRP, C-reactive protein; CVR, cerebrovascular resistance; FLAIR, fluid-attenuated inversion recovery; IR-FGR, inversion recovery fast gradient-recalled echo; MCA, middle cerebral artery; MCAl, left MCA; MCAr, right MCA; MRI, magnetic resonance imaging; sICAM-1, soluble intracellular adhesion molecule-1; TCD, transcranial Doppler ultrasound; WBC, white blood cell count; WMH, white matter hyperintensity.

References

1. Xu WL, Qiu CX, Wahlin A, Winblad B, Fratiglioni L. Diabetes mellitus and risk of dementia in the Kungsholmen project: a 6-year follow-up study. Neurology 2004;63:1181–1186. [PubMed: 15477535]
2. Harik SI, La Manna JC. Vascular perfusion and blood-brain glucose transport in acute and chronic hyperglycemia. J Neurochem 1988;51:1924–1929. [PubMed: 3183668]
3. Trauernicht AK, Sun H, Patel KP, Mayhan WG. Enalapril prevents impaired nitric oxide synthase-dependent dilatation of cerebral arterioles in diabetic rats. Stroke 2003;34:2698–2703. [PubMed: 14563973]
4. Makimattila S, Malmberg-Ceder K, Hakkinen AM, Vuori K, Salonen O, Summanen P, Yki-Jarvinen H, Kaste M, Heikkinen S, Lundbom N, Roine RO. Brain metabolic alterations in patients with type 1 diabetes-hyperglycemia-induced injury. J Cereb Blood Flow Metab 2004;24:1393–1399. [PubMed: 15625413]

5. Dandona P, James IM, Newbury PA, Woollard ML, Beckett AG. Cerebral blood flow in diabetes mellitus: evidence of abnormal cerebrovascular reactivity. Br Med J 1978;29:325–326. [PubMed: 687900]
6. Fulesdi B, Limburg M, Bereczki D, Kaplar M, Molnar C, Kappelmayer J, Neuwirth G, Csiba L. Cerebrovascular reactivity and reserve capacity in type II diabetes mellitus. J Diabetes Complications 1999;13:191–199. [PubMed: 10616858]
7. Kadoi Y, Saito S, Goto F, Fujita N. The effect of diabetes on the interrelationship between jugular venous oxygen saturation responsiveness to phenylephrine infusion and cerebrovascular carbon dioxide reactivity. Anesth Analg 2004;99:325–331. [PubMed: 15271699]
8. van Swieten JC, van den Hout JH, van Ketel BA, Hijdra A, van Gijn J. Periventricular lesions in the white matter on magnetic resonance imaging in the elderly: a morphometric correlation with arteriolosclerosis and dilated perivascular spaces. Brain 1991;114:761–774. [PubMed: 2043948]
9. deGroot JC, de Leeuw FE, Ouderk M, Hofman A, Jolles J, Breteler MM. Cerebral white matter lesions and subjective cognitive dysfunction: the Rotterdam Scan Study. Neurology 2001;56:1539–1541. [PubMed: 11402112]
10. Wahlund LO, Barkhof F, Fazekas F, Bronge L, Augustin M, Sjogren M, Wallin A, Ader H, Leys D, Pantoni L, Pasquier F, Erkinjuntti T, Scheltens P. A new rating scale for age-related white matter changes applicable to MRI and CT. Stroke 2001;32:1318–1322. [PubMed: 11387493]
11. Longstreth WT, Arnold AM, Beauchamp NJ Jr, Manolio TA, Lefkowitz D, Jungreis C, Hirsch CH, O'Leary DH, Furberg CD. Incidence, manifestations, and predictors of worsening white matter on serial cranial magnetic resonance imaging in the elderly: the Cardiovascular Health Study. Stroke 2005;36:56–61. [PubMed: 15569873]
12. Low PA. Evaluation of autonomic function. Curr Opin Neurol Neurosurg 1992;5:461–463. [PubMed: 1515685]
13. Aiello LM, Cavallerano JD, Cavallerano AA, Bursell SE. The Joslin Vision Network Innovative Telemedicine Care for Diabetes: preserving human vision. Ophthalmol Clin North Am 2000;13:213–224.
14. Cavallerano AA, Cavallerano JD, Katalinic P, Tolson AM, Aiello LM, Aiello LP, the Joslin Vision Netwrok Research Team. Use of Joslin Vision Network digital-video nonmydriatic retinal imaging to assess diabetic retinopathy in a clinical program. Retina 2003;23:215–223. [PubMed: 12707602]
15. Serrador JM, Picot PA, Rutt BK, Shoemaker JK, Bondar RL. MRI measures of middle cerebral artery diameter on conscious humans during simulated orthostasis. Stroke 2000;31:1672–1678. [PubMed: 10884472]
16. Novak V, Novak P, Schondorf R. Accuracy of beat-to-beat noninvasive measurement of finger arterial pressure using the Finapres: a spectral analysis approach. J Clin Monit 1994;10:118–126. [PubMed: 8207452]
17. Smith SM. Fast robust automated brain extraction. Human Brain Mapping 2002;17:143–155. [PubMed: 12391568]
18. Wells WM, Kininis R, Grimson WEL, Jolesz F. Adaptive segmentation of MRI data. IEEE Trans Biomed Eng 1996;15:429–442.
19. Dempster A, Laird N, Rubin D. Maximal likelihood from incomplete data via the EM algorithm. J R Stat Soc [Ser B] 1977;39:1–38.
20. Firbank MJ, Coulthard A, Harrison RM, Williams ED. Partial volume effects in MRI studies of multiple sclerosis. Magn Reson Imaging 1999;17:593–601. [PubMed: 10231186]
21. Woods RP, Grafton ST, Holmes CJ, Cherry SR, Mazziotta JC. Automated image registration. I. General methods and intrasubject, intramodality validation. J Comput Assist Tomogr 2005;22:139–152. [PubMed: 9448779]
22. Kadoi Y, Hinohara H, Kunimoto F, Saito S, Ide M, Hiraoka H, Kawahara F, Goto F. Diabetic patients have an impaired cerebral vasodilatory response to hypercapnia under propofol anesthesia. Stroke 2003;34:2399–2403. [PubMed: 12958324]
23. Marstrand JR, Garde E, Rostrup E, Ring P, Rosenbaum S, Mortensen EL, Larsson HB. Cerebral perfusion and cerebrovascular reactivity are reduced in white matter hyperintensities. Stroke 2002;34:972–976. [PubMed: 11935046]

24. Harris AK, Hutchinson JR, Sachidanandam K, Johnson MH, Dorrance AM, Stepp DW, Fagan SC, Ergul A. Type 2 diabetes causes remodeling of cerebrovasculature via differential regulation of matrix metal-loproteinases and collagen synthesis: role of endothelin-1. Diabetes 2005;54:2638–2644. [PubMed: 16123352]
25. Kario K, Ishikawa J, Hoshide S, Matsui Y, Morinari M, Eguchi K, Ishikawa S, Shimada K. Diabetic brain damage in hypertension: role of renin-angiotensin system. Hypertension 2005;45:887–893. [PubMed: 15824198]
26. Bouchard P, Ghitescu LD, Bendayan M. Morpho-functional studies of the blood-brain barrier in streptozotocin-induced diabetic rats. Diabetologia 2002;45:1017–1025. [PubMed: 12136401]
27. Tomassoni D, Bellagamba G, Postacchini D, Venarucci D, Amenta F. Cerebrovascular and brain microanatomy in spontaneously hypertensive rats with streptozotocin-induced diabetes. Clin Exp Hypertens 2004;26:305–321. [PubMed: 15195686]
28. El-Remessy AB, Al-Shabrawey M, Khalifa Y, Tsai NT, Caldwell RB, Liou GI. Neuro-protective and blood-retinal barrier-preserving effects of cannabidiol in experimental diabetes. Am J Pathol 2006;168:235–244. [PubMed: 16400026]
29. Wang P, Ba ZF, Chaudry IH. Administration of tumor necrosis factor-alpha in vivo depresses endothelium-dependent relaxation. Am J Physiol 1994;35:H2535–H2541. [PubMed: 8024016]
30. Makino N, Maeda T, Sugano M, Satoh S, Watanabe R, Abe N. High serum TNF-alpha level in type 2 diabetic patients with microangiopathy is associated with eNOS down-regulation and apoptosis in endothelial cells. J Diabetes Complications 2005;19:347–355. [PubMed: 16260352]
31. Schmidt MI, Duncan BB, Sharrett AR, Lindberg G, Savage PJ, Offenbacher S, Azambuja MI, Tracy RP, Heiss G. Markers of inflammation and prediction of diabetes mellitus in adults (Atherosclerosis Risk in Communities study): a cohort study. Lancet 1999;15:1649–1652. [PubMed: 10335783]
32. Duncan BB, Schmidt MI, Offenbacher S, Wu KK, Savage PJ, Heiss G. Factor VIII and other hemostasis variables are related to incident diabetes in adults: the Atherosclerosis Risk in Communities (ARIC) Study. Diabetes Care 1999;22:767–772. [PubMed: 10332679]

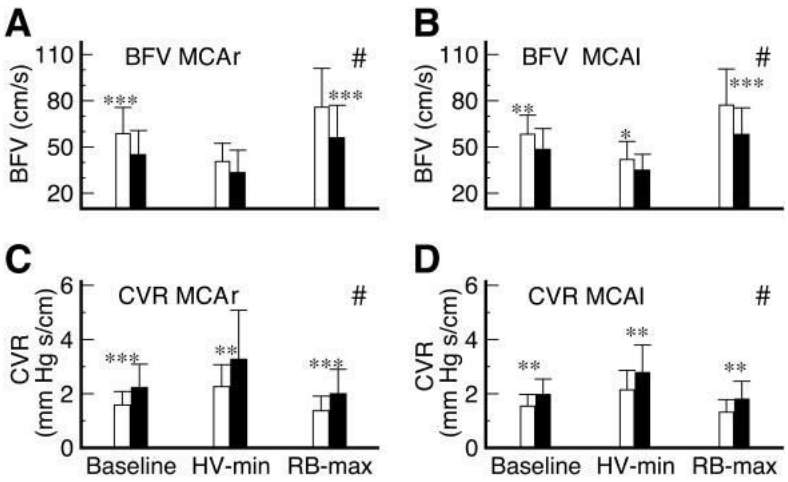

Figure 1.

*Comparisons of mean BFVs in the MCAr (A) and MCAl (B) and CVR in MCAr (C) and MCAl (D) during baseline, hyperventilation minimum (HV-minimum), and hyperventilation maximum (RB-maximum) during CO_2 rebreathing between the control (□) and diabetic (■) groups. Between-group comparisons for each condition at ***P ≤ 0.006, **0.006 < P ≤ 0.02, and *0.02 < P ≤ 0.05; comparisons between conditions at #P < 0.0001.*

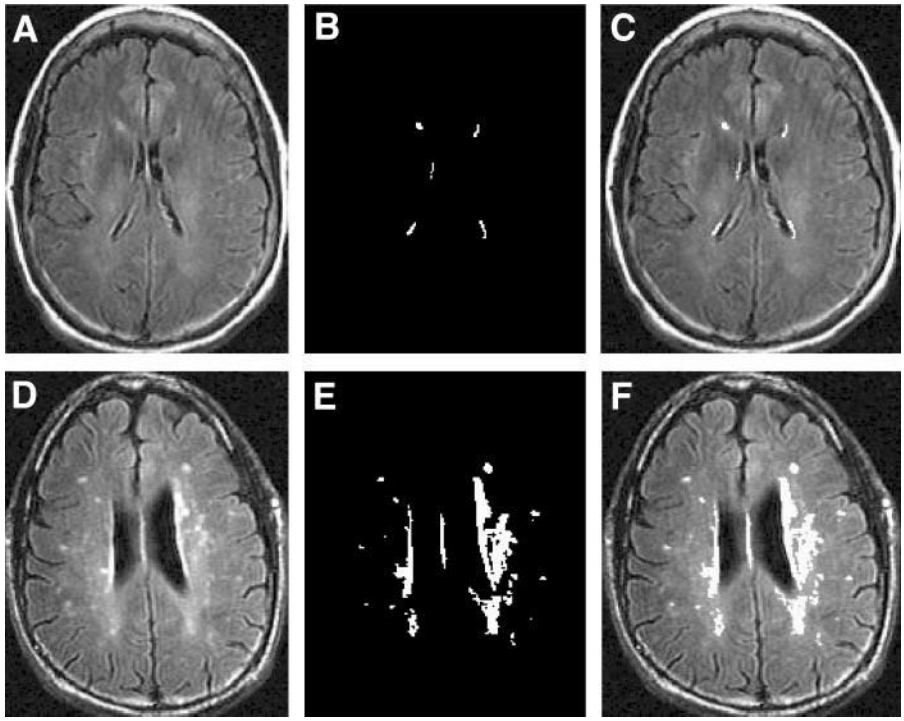

Figure 2.

*Axial slices at the level of the ventricles for a control (*A–C*) and a diabetic (*D–F*) subject. The three columns represent the FLAIR image (*A *and* D*), the WMHs segmentation (*B *and* E*), and the overlay of the segmentation on the FLAIR image (*C *and* F*).*

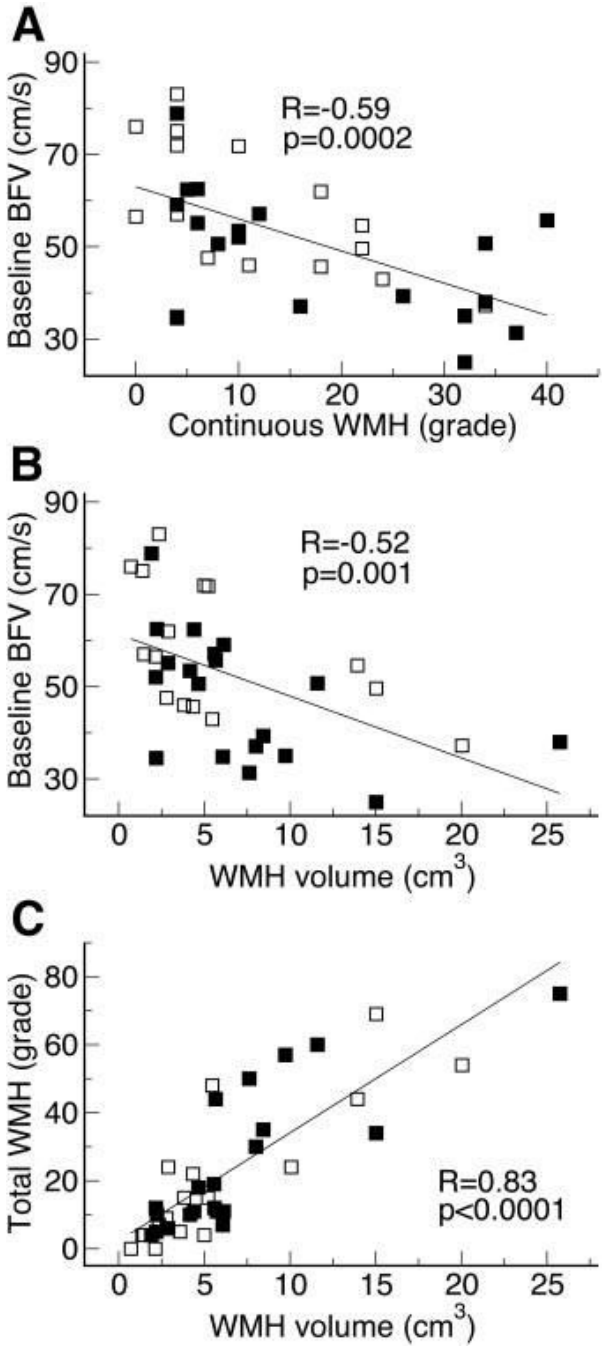

Figure 3.

*Relationship between baseline mean BFVs and sum grade of continuous WMHs on the visual rating scale (*A*) and WMH volume on MRI (*B*). Regression analysis revealing that BFV significantly declined with increased WMH grade and volume. Regression analysis between the WMH volume on MRI and sum of continuous and punctuate WMHs (total WMHs grade) on the visual rating scale (*C*) for control (□) and diabetic (■) subjects.*

Table 1

Characteristics of the study population

Group	Control	Diabetes	*P*
Age (years)	63.3 ± 7.6	61.5 ± 6.8	NS
Sex (male, female)	12, 10	16, 12	NS
Race (White, Asian, African American)	20, 1, 1	23, 2, 3	NS
BMI (kg/m^2)	24.4 ± 2.5	27.9 ± 4.6	0.002
Diabetes duration (years)		12.8 ± 11.5	
Hypertension (yes, no)	0, 22	10, 18	
Retinopathy (yes, no)	0, 12	10, 13	
Orthostatic hypotension (yes, no)	0, 22	5, 23	
Cardiac-vagal impairment (yes, no)	1, 21	12, 16	
Baseline heart rate (bpm)	65.1 ± 9.4	71.9 ± 11.9	0.03
Systolic blood pressure (mmHg)	120.3 ± 11.1	129.7 ± 17.1	0.03
Diastolic blood pressure (mmHg)	64.6 ± 10.4	64.9 ± 10.0	NS
Smoking (yes, no)	6, 16	11, 17	NS
Alcohol (yes, no)	17, 5	12, 16	0.01
A1C (%)	5.2 ± 0.4	7.3 ± 1.4	<0.0001
Glucose (mg/dl)	78.5 ± 17.0	130.7 ± 68.2	0.001
Triglycerides (mg/dl)	140.2 ± 73.6	235.2 ± 182.0	0.03
Total cholesterol (mg/dl)	224.1 ± 50.9	190.5 ± 41.4	0.02
HDL cholesterol (mg/dl)	66.6 ± 17.2	57.2 ± 15.8	0.05
LDL cholesterol (mg/dl)	131.0 ± 41.5	95.1 ± 29.2	0.001
WBC (K/**μ**l)	5.8 ± 1.2	7.3 ± 2.0	0.003
Urinary albumin (mg/dl)	3.0 ± 4.5	2.9 ± 4.4	NS
sICAM-1 (ng/ml)	209.5 ± 56.7	273.6 ± 118.8	0.05
sVCAM (ng/ml)	770.5 ± 183.5	800.6 ± 292.8	NS
CRP (mg/l)	2.3 ± 3.1	2.3 ± 2.0	NS
Interleukin-6 (pg/ml)	1.7 ± 0.4	2.2 ± 1.8	NS
Endothelin-1 (pg/ml)	0.8 ± 0.4	0.8 ± 0.2	NS
CO_2 reactivity MCAr ($cm \cdot s^{-1} \cdot mmHg^{-1}$)	1.61 ± 0.8	1.18 ± 0.7	0.05
CO_2 reactivity MCAl ($cm \cdot s^{-1} \cdot mmHg^{-1}$)	1.65 ± 0.7	1.28 ± 0.5	0.05
Vasodilatation reserve MCAr and MCAl (%)	41.7 ± 27.2	25.2 ± 15.0	0.04
Vasoconstriction reserve MCAr and MCAl (%)	−29.2 ± 9.5	−28.2 ± 14.6	NS

Data are means ± SD. *P* value denotes between-group comparisons. Vasodilatation/vasoconstriction reserve: % averaged MCAr and MCAl BFV increase/decrease between baseline and hypercapnia/hypocapnia. sVCAM, soluble vascular adhesion molecule.